Pharmacogn. Mag.
A multifaceted peer reviewed journal in the field of Pharmacognosy and Natural Products
www.phcog.com | www.phcog.net

ORIGINAL ARTICLE

Nanoencapsulation of *Tinospora cordifolia* (Willd.) Using Poly (D, L-lactide) Nanoparticles: Yield Optimization by Response Surface Methodology and *in silico* Modeling with Insulin Receptor Tyrosine Kinase

A. Ragavee, Selvaraj Asha Devi

Department of Biomedical Sciences, School of Bio Sciences and Technology, Vellore Institute of Technology, Vellore, Tamil Nadu, India

Submitted: 04-01-2019 Revised: 12-02-2019 Published: 26-08-2019

ABSTRACT

Background: *Tinospora cordifolia* (TC) is a widely used shrub in Ayurveda system of medicine. The main chemical constituent reported from this shrub is alkaloid with nitrogen heterocycles such as tropane alkaloids, thiazole, piperidines, and pyridine derivatives; nonisoprene indole alkaloids; and pseudoalkaloids with antidiabetic effects. **Materials and Methods:** The nanoparticles (NPs) were synthesized via solvent evaporation method using a biodegradable poly(D,L-lactide) (PLA) polymer. The NPs were then characterized using spectroscopic methods, X-ray diffraction, and scanning electron microscopy. Release profile and entrapment efficiency of the NPs are studied. Further, the synthesized NPs were evaluated for the inhibitory activity to find the antidiabetic potential and compared with docking analysis. **Results:** In this study, the TC extract was loaded to PLA NPs by the solvent evaporation method. The synthesis of NPs is sonicated at 40% amplitude at 30 s to get 48% of yield. The loading efficiency was found to be 76.21% for 5 mg and 58.10% for 10 mg. Release profile was observed with controlled release up to 8 h and 70% of TC was released after 40 h. Release kinetic showed good correlation with Higuchi kinetics. The maximum inhibitory percentage of TC-loaded PLA NPs was found to be 92.59 ± 0.854 and shows potential activity for diabetes. The interaction of the compounds with the receptor, fentanyl, and cholic acid showed that the highest binding energies of −6.09 and −6.4 have the potential to activate the insulin receptor. **Conclusion:** The result proves that TC stem extract possesses a therapeutic effect on diabetes and it is noticeable that acarbose interaction with insulin receptor shows minimum binding affinity when compared to the compounds from mass spectrum shows the highest binding affinity which acts as an insulin activator and responsible for the inhibitory action of α-glucosidase.

Key words: Molecular docking, poly(D,L-lactide), response surface methodology, solvent evaporation method, *Tinospora cordifolia*

SUMMARY

- TC-loaded poly(D,L-lactide) nanoparticles are synthesized by the solvent evaporation method
- The yield is optimized by altering the sonication parameters such as amplitude and time by response surface methodology
- Identification of bioactive compounds and validated using triple quadrupole LC-MS/MS analysis
- The *in silico* analysis showed the binding affinity of the ligand and receptor 1ir3 which proves the compound fentanyl and cholic acid was considered as the potent insulin activators.

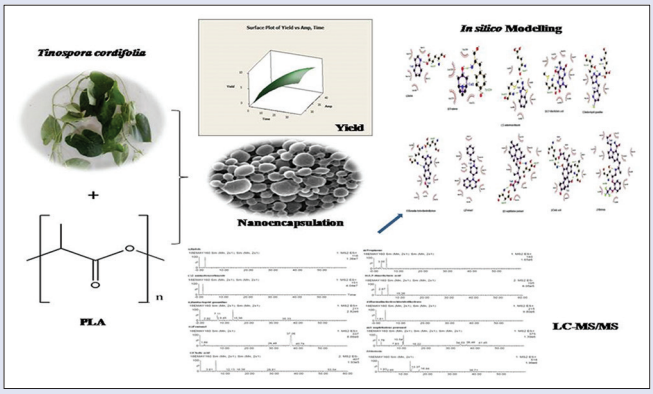

Abbreviations used: TC: *Tinospora cordifolia*; PLA: Poly(D,L-lactide); NPs: Nanoparticles; RSM: Response surface methodology; FFD: Full factorial design; CCD: Central composite design; ANOVA: Analysis of variance; PVA: Polyvinyl alcohol; DCM: Dichloromethane; LC-MS/MS: Liquid chromatography triple quadrupole mass spectrometry; FT-IR: Fourier-transform infrared spectroscopy; XRD: X-ray powder diffraction; HR-SEM High-resolution scanning electron microscopy; AFM: Atomic force microscopy; PDB: Protein data bank.

Correspondence:

Dr. Selvaraj Asha Devi,
Department of Biomedical Sciences, School of Bio Sciences and Technology, Vellore Institute of Technology, Vellore, Tamil Nadu, India.
E-mail: ashaselvaraj74@gmail.com

DOI: 10.4103/pm.pm_678_18

Access this article online
Website: www.phcog.com
Quick Response Code:

INTRODUCTION

Tinospora cordifolia (TC) (Willd.) Miers ex Hook.f. and Thoms is a prodigious, barren, ephemeral climbing shrub belonging to the family Menispermaceae and order Ranunculales.[1] The plant is indigenously known as guduchi, giloy, amruthaballi, and shindilakodi and is extensively distributed in India. This plant is described as a large, deciduous, abundant, spreading, climbing shrub with elongated twining branches. The stems of TC are rather succulent with long filiform fleshy aerial roots from the branches. The leaves are membranous and cordate.

Cite this article as: Ragavee A, Devi SA. Nanoencapsulation of *Tinospora cordifolia* (Willd.) using poly (D, L-lactide) nanoparticles: Yield optimization by response surface methodology and *in silico* modeling with insulin receptor tyrosine kinase. Phcog Mag 2019;15:S218-27.

The flowers are small and yellow or greenish yellow; the male flowers are clustered and the female flowers are usually solitary. The fruits aggregate of 1–3, smooth drupelets with ovoid shape on a thick stalk with subterminal style scars, scarlet, or orange colored.[2] The stem and root of TC are predominantly practiced in ayurvedic and ancestry medicine. It is known for its general tonic, anticancer, antiarthritic, antihyperglycemic, and anti-inflammatory properties.[3] Anti-inflammatory activity of this plant is evaluated by carrageenan-induced paw edema, and the inflammation is suppressed by the octacosanol as reported.[4] The antiarthritic activity of TC has been studied with induced adjuvant model in animals, and the proinflammatory cytokines are greatly reduced spleen adherent cells and draining lymph node cells of animals treated with TC crude extract.[5] The stem extracts of TC are rich in isoquinoline alkaloid which helps in releasing insulin, so it is extensively used for treating diabetes.[6] The water-dispersible alkaloids such as berberine, palmatine, tinosporine, and isocolumbine are present in this plant, which acts as a glucosidase inhibitor.[7] This plant is rich in alkaloids, phenols, glycosides, aliphatic compounds, and natural polymers such as mucilages and gums.[8] The other phytocompounds reported recently from methanolic stem extracts of TC are cetyl alcohol, three cinnamoylnaphthyl amides, naphtholdiarabinosyl alkanes, geranilanoatearabinoside, and labdenyl flavanone and biological activity of these compounds are unknown need to be studied in future.[9]

Diabetes mellitus is a disease caused due to the defects in insulin secretion, insulin action, or both, which will increase the blood glucose level. The elevated blood glucose level causes serious complications and affects various organs such as eyes, heart, nerves, kidneys, and blood vessels. Diabetes mellitus can be managed by chemical drugs; however, these drugs have been reported to have various side effects. Hence, as an alternative remedy, a large number of medicinal plants, widely recognized as an important source of drugs, have been used to treat diabetes because these natural products have lesser toxic effects. It is also estimated that about 80% of diabetics around the world population presently depend on the herbal medicine for their successful treatments.[10] Based on the previous reports on multipurpose therapeutic effect of TC phytoconstituents, this plant has been chosen for the study. In this study, polymers are used as an entrapment ingredient for the release of the compound, which acts as prodrug or drug carriers. Numerous biodegradable polymeric nanoparticles (NPs) have been broadly used for the delivery of molecules and drugs.[11-13] The proficiency of polymeric NPs acts as a carrier of drugs to target sites by reducing the adverse side effects.[14] Diverse biodegradable polymers such as Poly (D,L-lactide) (PLA), Poly (lactic-co-glycolic acid) (PLGA), Poly (ε-caprolactone), gelatine, chitosan, and gelatine Poly (alkyl cyanoacrylates) have been notably used for targeted delivery of drugs associated with diabetes, cancer, asthma, malaria, and other malignant diseases.[15-19] PLA and PLGA are mostly used in the synthesis of NPs and approved in a parental application by the Food and Drug Administration.[20] Among many biodegradable polymers, PLA has been substantially used for the encapsulation of therapeutic agents relevant to its high biodegradability, low toxicity, biocompatibility, bioavailability, and prolonged drug release.[21-24]

The hypothesis behind this study was to analyze the encapsulation efficiency of TC-loaded PLA NPs, and its glucosidase inhibition percentage was studied for synthesized NPs to screen the potential antidiabetic activity. The *in silico* docking analysis was performed for the compound reported in the mass spectrum of liquid chromatography triple quadrupole mass spectrometry (LC-MS/MS) of the TC stem extract and insulin receptor to screen the best interaction, thereby regulating blood glucose through insulin signaling.

MATERIALS AND METHODS

Chemicals

PLA (MW: 75,000–120,000), polyvinyl alcohol (PVA), and berberine chloride were procured from Sigma-Aldrich, USA. Dichloromethane (DCM) and dialysis bag were purchased from HiMedia Laboratories Ltd.

Preparation of plant extract

TC stem was collected from Vellore District, Tamil Nadu, India, and was authenticated from the Plant Anatomy Research Centre (PARC/2018/3808). The stem was dried and ground to a coarse powder. The stem powder was mixed with distilled water and stirred magnetically overnight (12 h) at room temperature.[25] This was repeated three consecutive times. The residue was removed by filtration, and the extract was lyophilized for further use.

Characterization of *Tinospora cordifolia*

The Fourier-transform infrared (FT-IR) analysis of the extract was used to determine the functional groups present in it. For the analysis, the lyophilized TC stem extract powder recorded on KBr disk was used for scanning range of 400–4000 cm^{-1} and at 1 cm^{-1} resolution. The spectra were recorded on FT-IT Bruker spectroscope using the sampler accessory. LC-MS analysis of the TC extract was done primarily to identify the total ion chromatogram (TIC) and followed by triple quadrupole LC-MS/MS analysis of the extract was performed on an Agilent connected to a system via electricity ionization (XEVO-TQD#QCA1232, USA). The separation was carried out on a SUNFIRE C-18, column (250 mm × 4.6 mm, 5 µm) with 1 ml/min flow rate followed by gradient programming. The diode array recorded ultraviolet (UV) spectrum at 280 nm.

Experimental design

A full factorial design (FFD) was used to investigate the individual variables such as sonication time (sec) and amplitude of sonication (Amp) to find the effect on the responses of TC-loaded PLA NP yield (%). Test values were chosen based on the literature.[26,27] From the effects of FFD, a central composite design (CCD) was made utilizing the same independent variables. The impact of independent variables on the responses of TC-loaded PLA NP yield was examined by the response surface methodology (RSM) using a commercial statistics package: Minitab version 16 (Minitab Inc., Pennsylvania, U.S.A), and the optimized condition was used to synthesize the TC-loaded PLA NPs. The regression coefficient was found using multiple linear regressions. The significance was found in the analysis of variance (ANOVA).

Synthesis of poly(D,L-lactide) nanoparticles using *Tinospora cordifolia* extract

TC-loaded PLA NPs were synthesized using a solvent evaporation method[28] and based on the optimization of FFD. 50 mg of PLA and 5 mg of the dried TC stem extract were sonicated (Sonics and Materials, INC.53, Church Hill Road, New Town, CT, USA, Model-VCX500) together at 40% amplitude in 2 mL of DCM solution for 30 s at room temperature. 4 mL (1%) of PVA solution was added again and sonicated to form an emulsion. Further, the emulsion was diluted with PVA solution (0.1%) to make up the volume to 80 ml, and the organic solvent DCM present in the emulsion was evaporated by stirring for 3 h. After stirring, the solution was centrifuged at 16,500 rpm for 10 min at 10°C and washed thrice with distilled water. The resulting NPs were lyophilized

using a lyophilizer (Lark Innovative Fine Teknowledge, India) and stored at 2°C–8°C till further use.

Characterization of synthesized nanoparticles

Lyophilized TC-loaded PLA NP powder was recorded on KBr plates in a scanning of 400–4000 cm^{-1} at 1 cm^{-1} resolution. The spectral data were recorded and analyzed on FTIR (IR Affinity-1, Shimadzu, Japan) to determine the functional groups, encapsulated on the synthesized NPs. XRD analysis was used to find the phase identification of the TC-loaded PLA NPs. The peak was observed using XRD (Bruker D8 Advance, Germany). The surface and morphology and the structure of TC-PLA NPs were observed using the F E I Quanta FEG 200 high-resolution scanning electron microscopy (HR-SEM). Atomic force microscopy (AFM) was used to get the elucidated surface image of TC-loaded PLA NPs. The observations were made in an AFM (Nanosurf, Switzerland) at static force operating mode using a cantilever type ContAl-G. The size distribution and zeta potential of synthesized NPs were analyzed in a nanosizer (Horiba SZ-100). Lyophilized TC-PLA NPs were suspended in Milli-Q water and homogenized. The size distribution of the particle was determined through the principle of dynamic light scattering in glass cuvettes. To estimate the agglomerates, homogenized NP solution was filtered using a 1-μm glass microfiber filter. To measure the zeta potential, 2 mL of the solution was used with cuvettes.

Percentage yield

The yield of TC-loaded PLA NPs was calculated using the following formula:

$$\text{Yield}(\%) = \frac{\text{Mass of nanoparticles obtained}}{\text{Total weight of TC + PLA}} \times 100$$

Percentage entrapment efficiency of *Tinospora cordifolia* poly(D,L-lactide) nanoparticles

The entrapment efficiency of the TC-PLA NPs after the synthesis was determined as the difference between the amount used to prepare the NPs and the amount found in the supernatant. The total alkaloid content in the NPs was estimated using bromocresol green method.[29] The total alkaloid contents in TC-loaded PLA NPs were expressed in terms of berberine chloride equivalent with a standard curve, and the loading efficiency was calculated using the following formula:

$$\text{EE}(\%) = \frac{\text{Amount of TC entrapped}}{\text{Total amount of TC}} \times 100$$

In vitro release profile

In vitro release of TC from PLA NPs was estimated by the dialysis bag diffusion method.[30] The TC-loaded PLA NP (1 mg/ml) was placed in the dialysis bag, which was sealed at both the ends. The dialysis bag was immersed in phosphate-buffered solution (PBS) of pH 7.4, which was stirred at 200 rpm at room temperature, and the samples were withdrawn at every 1 h time interval from 0 h to 40 h, and the same volume was replaced by fresh PBS. The samples were then analyzed using a UV-Vis spectrophotometer.

Mathematical model and release kinetics

The *in vitro* TC-loaded PLA NP (1 mg/ml) profile was fitted to various mathematical models to determine the release kinetics mechanism such as zero-order, first-order, and Higuchi models.[31] The best fit for each model was evaluated by the correlation coefficient value (R^2), and the mechanism of release was determined by the release exponent value (n) based on Korsmeyer–Peppas model.[32]

α-Glucosidase inhibitory activity

Alpha-glucosidase percentage inhibition activity of synthesized TC-loaded PLA NPs was determined by the standard method.[33] The assay was performed in a 96-well plate, and the reaction mixture contains 50 μl of phosphate buffer (100 mM, pH 6.8), 10 μl of alpha-glucosidase (1 U/ml), and 20 μ1 of varied concentrations of synthesized NPs (200, 400, 600, 800, and 1000 μg/ml). The mixture was incubated at 37°C for 10 min, and P-NPG substrate (5 mM) was added and further incubated for 37°C for 20 min. The reaction was stopped by adding 50 μl of Na_2CO_3 (0.1 M). The absorbance of the released p-nitrophenol was measured at 405 nm. Acarbose is used as a standard with varying concentrations (200, 400, 600, 800, and 1000 μg/ml). The control was performed without test sample, and the percentage inhibition was calculated using the following formula:

$$\%\,\text{Inhibiton} = 1 - \frac{\text{Absorbance of test}}{\text{Absorbance of control}} \times 100$$

In silico molecular docking

The molecular docking analysis was performed to study the interaction of bioactive compounds with the insulin receptor. Insulin receptor associates to the class of tyrosine kinase receptor. The binding of insulin receptor causes structural changes in the receptor which leads to stimulate the tyrosine kinase beta subunit.[34] The compounds are screened based on the mass spectrum obtained from LC-MS/MS. The receptor file was downloaded from the Protein Data Bank. Structures of the predicted compounds (ligands) were obtained from PubChem. The interaction between the compound and the receptor was analyzed using AutoDock 4. The best interaction was chosen with minimum docked energy, and the hydrogen bonds formed were analyzed using LigPlot.

RESULTS

Characterization of *Tinospora cordifolia*

FT-IR spectroscopy analysis was carried out to determine the functional groups of phytocompounds present in the TC stem extract. The interpretations of compounds were done using standard infrared charts. In TC stem extract the major peak showing (O-H) stretch with broad curve representing the alcohol group at 3329.14, followed by the (C-H) stretch of alkanes at 2922.16, aldehydes (C = O) at 1734.01 and amines N-H bond at 1625.99, peak 1514.12 shows the nitro compound with asymmetric stretch, alkanes (C-H) and (C-O) stretch carboxylic acids, esters were found at 1369.46 and 1317.38. The aliphatic amines (C-N) stretch at 1230.58, followed by the (C-Cl), (C-Br) stretch of alkyl halides at 1024.20, 779.24, 597.93, and 516.92, respectively, were found [Figure 1a]. These results clearly indicate the presence of alkaloids in the TC stem extract. Further, it is confirmed by the mass spectrum analysis.

Liquid chromatography triple quadrupole mass spectrometry analysis of *Tinospora cordifolia*

The LC-MS analysis of TC extract represents the TIC [Figure 2], and for further specificity of compound, LC-MS/MS is rendered. The compounds were identified by the MassBank of North America based on the precursor m/z, precursor type, retention time, and mode of ionization [Figure 3]. The compounds were separated by SUNFIRE C-18 column. In positive ionization mode, the protonated molecular ions $[M + H]^+$ were observed at m/z 118, 140, 151, 211, 215, and 337 for indole, tropinone, 2-aminobenzothiazole, imidacloprid–guanidine,

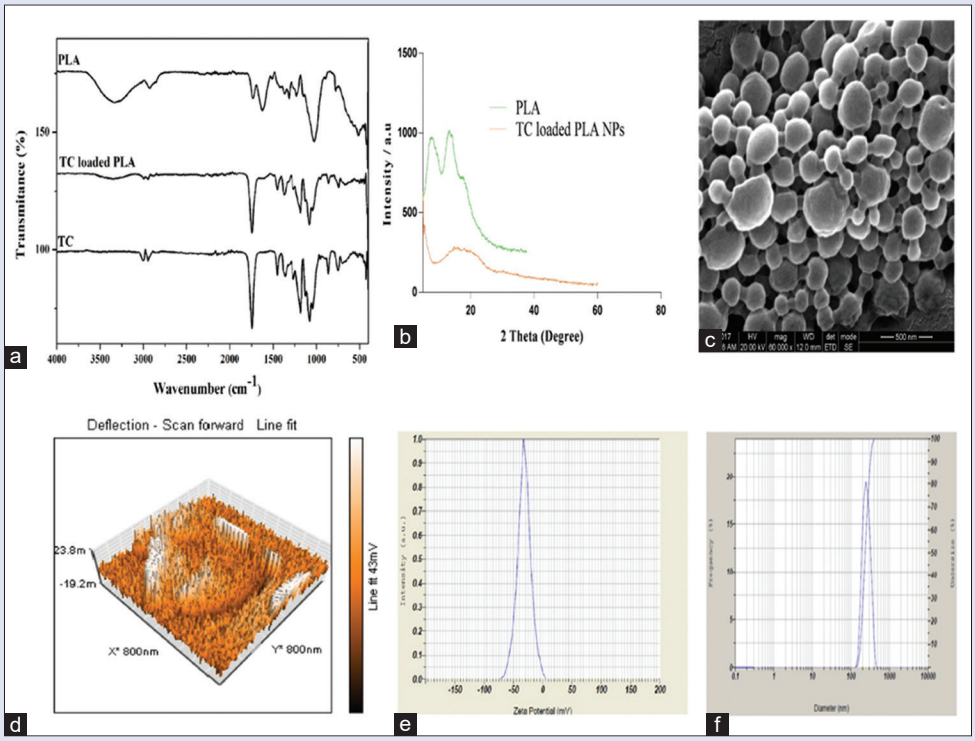

Figure 1: Characterization of TC-loaded PLA NPs. (a) FT-IR spectra of TC, TC-loaded PLA NPs, and PLA. (b) XRD analysis of TC-loaded PLA of TC-loaded NPs. (c) HR-SEM of TC-loaded PLA NPs. (d) AFM images of TC-loaded NPs. (e) Zeta potential. (f) Particle size of TC-loaded PLA NPs. NPs: Nanoparticles; TC: *Tinospora cordifolia*; PLA: Poly(D,L-lactide); FT-IR: Fourier-transform infrared; XRD: X-ray powder diffraction; HR-SEM: High-resolution scanning electron microscopy; AFM: Atomic force microscopy

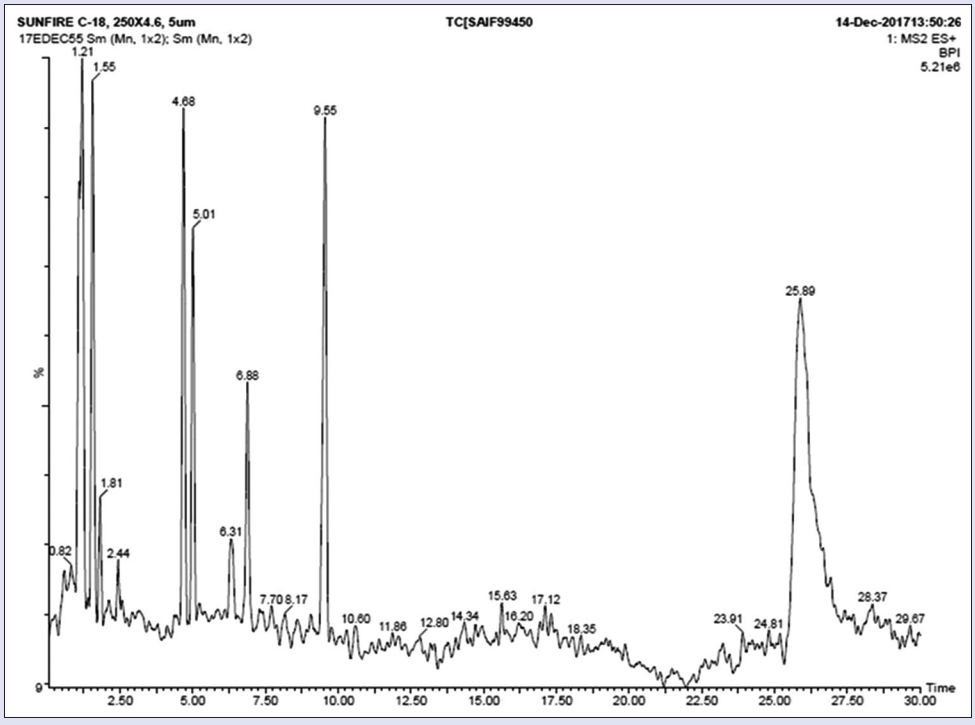

Figure 2: Liquid chromatography mass spectrometry analysis of *Tinospora cordifolia* extract represents the total ion chromatogram

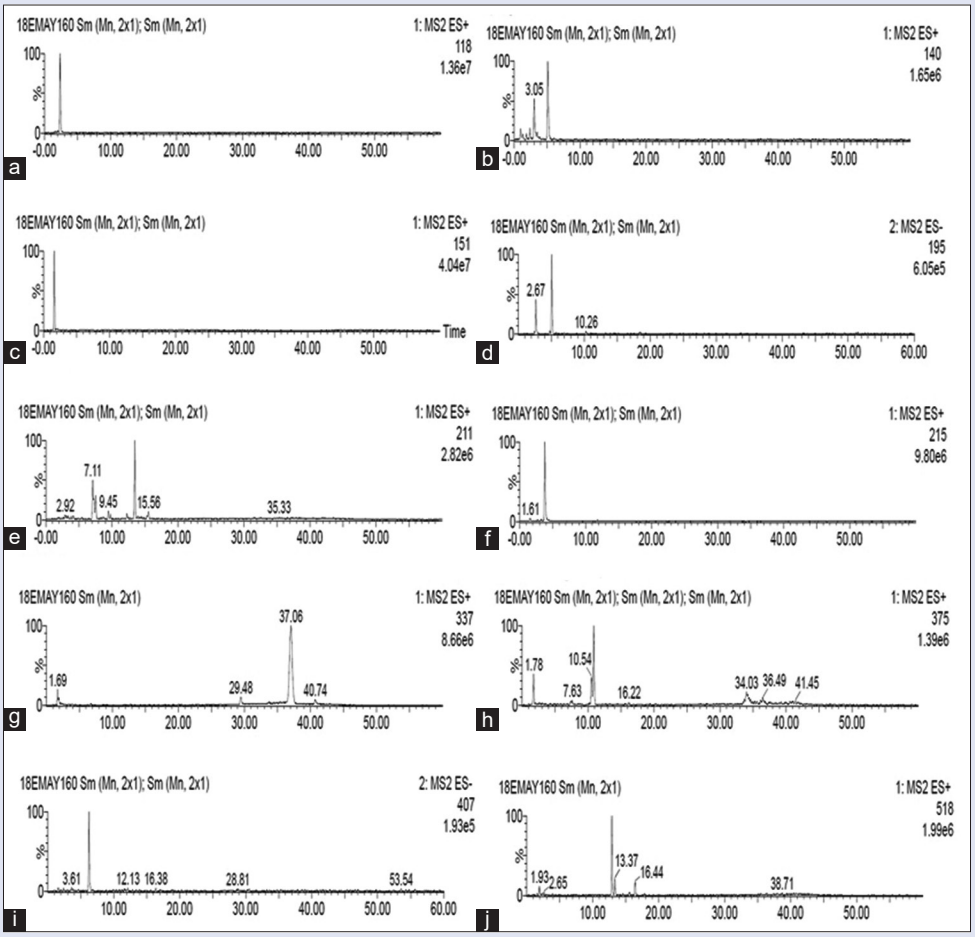

Figure 3: LC-MS/MS of TC extract. (a) Indo, (b) Tropinone, (c) 2-aminobenzothiazole, (d) 1,9-dimethyluric acid, (e) imidacloprid–guanidine, (f) harmaline hydrochloride dihydrate, (g) fentanyl, (h) 1-naphthalene pentanol, (i) cholic acid, (j) silodosin. LC-MS/MS: Liquid chromatography triple quadrupole mass spectrometry; TC: *Tinospora cordifolia*

harmaline hydrochloride dehydrate, and fentanyl, respectively. Sodiated molecular ions $[M + Na]^+$ were noted at m/z 375 and 518 for 1-naphthalene pentanol and silodosin, respectively. The negative ionization mode $[M-H]^-$ at m/z 195 and 407 for 1,9-dimethyluric acid and cholic acid, respectively [Table 1].

Experimental design

An FFD model was conducted to study the effect of the design variables of TC-loaded PLA NP yield. After implementing the FFD, RSM was executed using a CCD with design variables (sonication time and amplitude) to scrutinize its effect on the responses. The design variables with the actual and coded levels and the responses of the FFD and CCD are indicated in Table 2. The TC-loaded PLA NP yield ranged between 8.5% and 48% for FFD with the highest yield (%) at 40% amplitude for 30 s. The data acquired from CCD were found to be 8.7%–48% with the highest percentage at 40% amplitude for 30 s.

Table 3 denotes the regression coefficients of the statistical model built based on the CCD. The linear and quadratic effects of amplitude and correlation between amplitude and time had no impact on TC-loaded PLA NP yield ($P > 0.05$). However, the correlation between the variables such as time and amplitude was found to be statistically significant ($P < 0.05$). The correlation coefficient of time was found to be positive, indicating that higher TC-loaded PLA NP yield was obtained at a higher time. The linear effect of time was found to be statistically significant ($P < 0.05$) for TC-loaded PLA NP yield.

The equation shows the statistical model built for TC-loaded PLA NP yield:

$$Yield(\%) = 40.15 - 3.35\,\text{Amp} + 23.77\,\text{Time} - 8.58\,\text{Amp}^2 - 17.83\,\text{Time}^2 + 0.4\,\text{Amp} \times \text{Time}$$

ANOVA was performed for the statistical model [Table 4], and the regression was found to be statistically significant ($P < 0.05$) with an increase in time. Hence, it is proved that the executed model is fit and can be used to predict the surface, and contour plots for the responses will be built based on the interpretation of the coefficient's yield. Figure 4a and b interprets the surface and contour plots built for the TC-loaded PLA NP yield (time, amplitude). It follows the stationary, rigid response surface pattern. According to this pattern, the response (TC-loaded PLA NP yield) increases with time. From the 2D and 3D plots, it is proved that the increase in time and amplitude would increase the yield of TC-loaded PLA NPs. As a result, the recommended condition is 40% amplitude at 30 s to obtain 48% yield based on 1:2 of TC and PLA, respectively. Therefore, PLA NP encapsulation efficiency on the plant extracts help obtain biodegradable NPs for controlled release of TC extract.

Table 1: Mass fragmentation of compounds identified

Retention time	m/z	Ionization mode	Precursor type	Formula	Compound	Structures
2.369	118	Positive	$[M+H]^+$	C_8H_7N	Indole	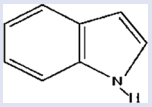
5.007	140	Positive	$[M+H]^+$	$C_8H_{13}NO$	Tropinone	
1.64	151	Positive	$[M+H]^+$	$C_7H_6N_2S$	2-aminobenzothiazole	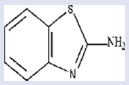
5.033	195	Negative	[M-H]	$C_7H_8N_4O_3$	1,9-dimethyluric acid	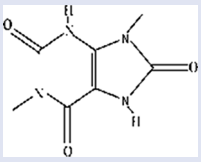
13.44	211	Positive	$[M+H]^+$	$C_9H_{11}ClN_4$	Imidacloprid–guanidine	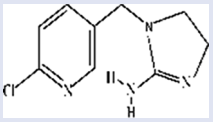
3.79	215	Positive	$[M+H]^+$	$C_{13}H_{14}N_2O$	Harmaline Hydrochloride dihydrate	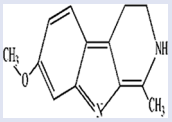
37.11	337	Positive	$[M+H]^+$	$C_{22}H_{28}N_2O$	Fentanyl	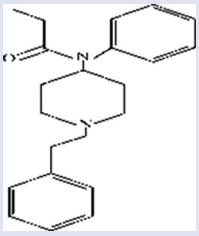
10.89	375	Positive	[M+Na]	$C_{22}H_{40}O_3$	1-naphthalene pentanol	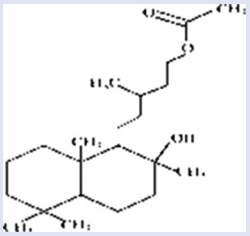
6.3	407	Negative	$[M-H]^-$	$C_{24}H_{40}O_5$	Cholic acid	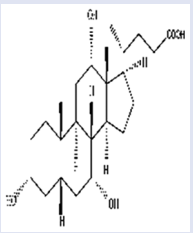
12.92	518	Positive	[M+Na]	$C_{25}H_{32}F_3N_3O_4$	Silodosin	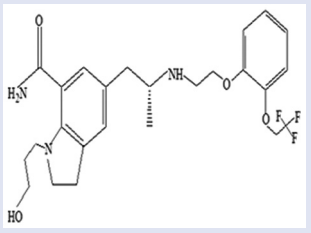

Table 2: Full factorial design and central composite design for the independent variables (actual and coded levels) and the responses

FFD			
Run	**Time (s)**	**Amplitude (%)**	**Yield (%)**
1	30 (+)	40 (+)	48.0
2	5 (−)	40 (+)	10.0
3	30 (+)	30 (−)	45.0
4	5 (−)	30 (−)	8.5
CCD			
1	17.50 (0)	35.00 (0)	40.12
2	17.50 (0)	27.92 (−1)	38.40
3	17.50 (0)	35.00 (0)	40.00
4	10.00 (−)	35.00 (0)	15.00
5	17.50 (0)	42.07 (+1)	22.30
6	17.50 (0)	35.00 (0)	40.40
7	30.00 (+1)	40.00 (+1)	48.00
8	5.00 (−1)	30.00 (−1)	8.70
9	5.00 (−1)	40.00 (+1)	10.20
10	30.00 (−1)	30.00 (−1)	45.70
11	17.50 (0)	35.00 (0)	40.23
12	17.50 (0)	35.00 (0)	40.00
13	35.17 (−1)	35.00 (0)	42.20

FFD: Full factorial design; CCD: Central composite design

Table 3: Regression coefficient estimates for central composite design and statistical analysis for *Tinospora cordifolia* loaded poly(D,L-lactide) nanoparticle yield (%)

Variables	Regression coefficient	SE	*t*	*P*
Constant	40.15	1.918	20.938	0.000
Amp (L)	−3.3532	2.144	−1.564	0.162
Time (L)	23.7729	2.144	11.089	0.000
Amp (Q)	−8.5875	3.251	−2.641	0.033
Time (Q)	−17.835	3.251	−5.486	0.001
Amp × ime	0.4000	4.288	0.093	0.928

SE: Standard error; Amp: Amplitude

Table 4: Analysis of variance for fitted models (yield percentage)s

Source	Df	SS	MS	*F*	*P*
Regression	5	2928.44	585.69	31.86	0.000
Linear Amp × time	1	2305.58	1152.79	62.70	0.000
Amp × amp	1	69.35	128.25	6.98	0.033
Time × time	1	553.35	553.35	30.10	0.001
Interaction Amp × time	1	0.16	0.16	0.01	0.928
Residual error	7	128.69	18.38		
Lack of fit	3	128.58	42.86	1493.34	0.000
Pure error	4	0.11	0.03		
Total	12	3057.13			

DF: Degree of freedom; SS: Sums of squares; MS: Mean squares; Amp: Amplitude

Characterization of *Tinospora cordifolia*-loaded poly(D,L-lactide) nanoparticles

The phytocompounds from the stem extract capped onto synthesized NPs were confirmed by FT-IR spectroscopy matching the acquired spectrum with a reference spectrum. The major peak showing (O-H) stretch with broadband representing the alcohol group at 3350.35, followed by the (C-H) stretch of alkanes at 2945.30, (C = O) stretch of esters at 1745.58 and C-H bond at 1450.47 forms alkanes, 1373.32 peak shows nitro groups and 1184.29 forms alkyl halides and (C-N), (C-H), stretch of aliphatic and aromatic amines at 1045.42, 862.18 and 744.52 respectively were found. The FT-IR spectrum of synthesized

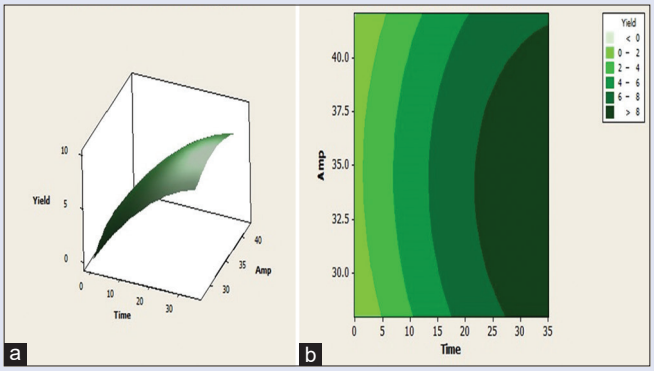

Figure 4: (a) Surface plot of yields versus amplitude and time. (b) Contour plot of yield versus amplitude and time

TC-loaded NPs confirmed the encapsulation of polymer on TC extract by a difference in the peak transmittance (%) when compared with neat PLA [Figure 1a]. The XRD analysis of TC-loaded PLA NPs showed peak at 14.8 – (1 0 1) lattice, 16.8 – (0 2 0) lattice, 19.1 (0 2 3) lattice, 22.3 – (1 2 2) lattice. The XRD pattern predicted the amorphous structure of TC-loaded PLA NPs when compared with PLA [Figure 1b]. The HR-SEM image revealed the spherical nature of TC-loaded PLA NPs, and the size was found to be 236.8 nm [Figure 1c]. AFM topography images of TC-loaded PLA NPs sample deposited on mica demonstrated the presence of spherical flattened particles, with root mean square at 308 nm [Figure 1d]. The zeta potential value of the TC-loaded PLA NPs was −28.0 mV, which predicted the stable nature of NPs [Figure 1e]. Particle size analyzer shows 232.5 nm at 90° scattering angle based on the principle of scattered light intensity [Figure 1f]. Polydispersion index values were under 0.2, representing the monodispersion of the particles in the nanosize range.

Yield percentage

The yield percentage for synthesized TC-loaded PLA NPs in the ratio of 1:2, i.e., 500 mg of TC and 1000 mg of PLA, was found to be 48%, which is synthesized based on the optimized condition using the RSM.

Entrapment efficiency

The entrapment efficiency was measured by the total alkaloid contents in TC-loaded PLA NPs and expressed in terms of berberine chloride equivalent as a standard curve. The loading efficiency for 5 mg of TC-PLA NPs was 76.21%, and for 10 mg of TC-PLA NPs, it was 58.10%.

In vitro release profile

In vitro release of TC from PLA NPs was performed in physiological conditions at pH 7.4 over a period of 40 h [Figure 5]. The release profile for 1 mg/ml concentration of TC-loaded PLA NPs displayed a controlled release up to 8 h, and sudden release at 12 h was observed and the 70% of TC was released after 40 h.

Mathematical model and kinetics release mechanism

The *in vitro* TC-loaded PLA NP (1 mg/ml) release profile was fitted to various mathematical models to determine the release kinetics mechanism. The best fit for each model was evaluated by the correlation coefficient value (R^2), and release kinetic constant showed good correlation with Higuchi kinetics [Table 5] and the value of release exponent (n) showed Fickian diffusion.

α-Glucosidase inhibitory activity

In vitro antidiabetic activity of TC-loaded PLA NPs was determined by alpha-glucosidase inhibitory assay. The synthesized NPs showed potential inhibitory activity when compared to the standard. The percentage of inhibition in the TC-loaded PLA NPs was dose dependent, and the maximum inhibitory percentage was 92.59 ± 0.854 whereas the maximum percentage inhibition of the standard acarbose was 98.37 ± 0.70 at a concentration of 1000 µg/ml [Figure 6a]. The phytoconstituents present in the plant as the potential to reduce the blood glucose level.

In silico analysis

The prediction of compounds with reference to mass spectrum was obtained from MassBank of North America. PDB structures obtained from PubChem were docked with the insulin receptor 1ir3, which shows the binding energy at kcal/mol and formation of hydrogen bond with active site residues [Figure 7]. Based on the interaction of the compounds with receptor, cholic acid observed to interact with the active residue site at LYS1165; LEU1171 showed the highest binding energy of −6.4 and fentanyl at −6.09 have the potential to activate the insulin receptor [Table 6]. Glucosidase inhibitor (acarbose) interaction with receptor showed interaction with residue site at ASP1083; LEU1002; GLU1043 and minimum binding energy of −3.2 were observed. The correlation of glucosidase inhibitor with insulin receptor showed minimal binding affinity when compared to the compounds such as cholic acid and fentanyl, which showed the maximum binding energy and efficient to activate insulin receptor [Figure 6b].

Table 5: Mathematical model and kinetics release mechanism

Kinetic model	Correlation coefficient (R^2)	Kinetic constant (k)
Zero order	0.961	K_0=0.866
First order	0.948	K_1=0.391
Higuchi	0.96	K_H=0.86
Kinetic model	Release exponent (n)	Drug transport mechanism
Korsmeyer–Peppas	n=0.110	Fickian diffusion

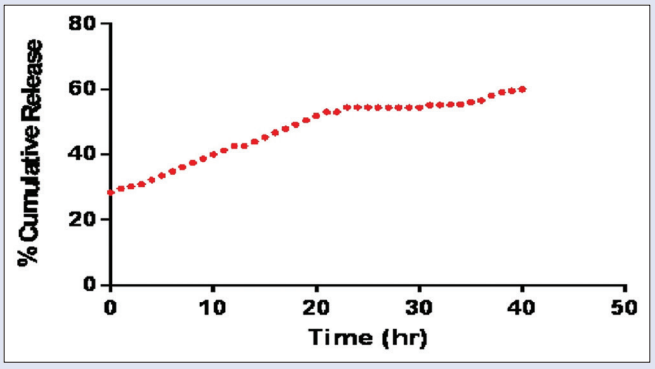

Figure 5: *In vitro* release profile of *Tinospora cordifolia* from Poly (D, L-lactide) nanoparticles

DISCUSSION

The polymeric NPs were used as drug delivery molecules due to the properties such as biodegradability, biocompatibility, high stability and encapsulation efficiency, and sustained release effect.[35,36] In this study, the TC stem extract was prepared, and polymeric TC-loaded PLA NPs were synthesized using a solvent evaporation method. The FTIR analysis of the extract showed that a major curve corresponds to an alcohol group which is further confirmed by LC-MS/MS analysis. The insulin receptor undergoes the conformational changes by activating the tyrosine kinase beta submit and induces glucose uptake in cells.[37] Binding of insulin and activates protein, which regulates glycogen synthesis and minimizes the blood glucose level. The FT-IR spectrum of synthesized TC-loaded PLA NPs confirms the encapsulation of polymer with TC extract and revealed the presence of alkaloids. The XRD pattern predicted the amorphous structure of synthesized NPs, and the zeta potential value of the NPs was −28.0 mV, implying the good stability of the nanoformulation. The SEM image confirmed the spherical nature of NPs, and the size was found to be 236.8 nm. The size and shape of NPs directly influenced their cellular uptake, which was accompanied in the cell by endocytosis process.[38] TC release from PLA NPs through the dialysis membrane displayed a controlled release up to 20 h, and release kinetic constant showed good correlation with Higuchi kinetics. A drug release study proved that the nanoformulations have a sustained release profile compared

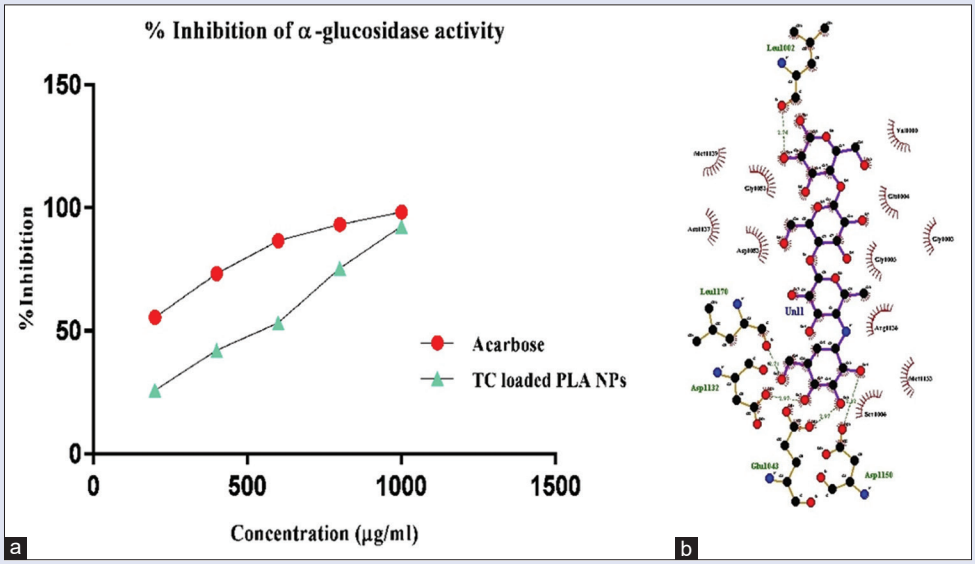

Figure 6: (a) Percentage inhibition of α-glucosidase activity; (b) ligplot analysis – interaction of acarbose with insulin receptor

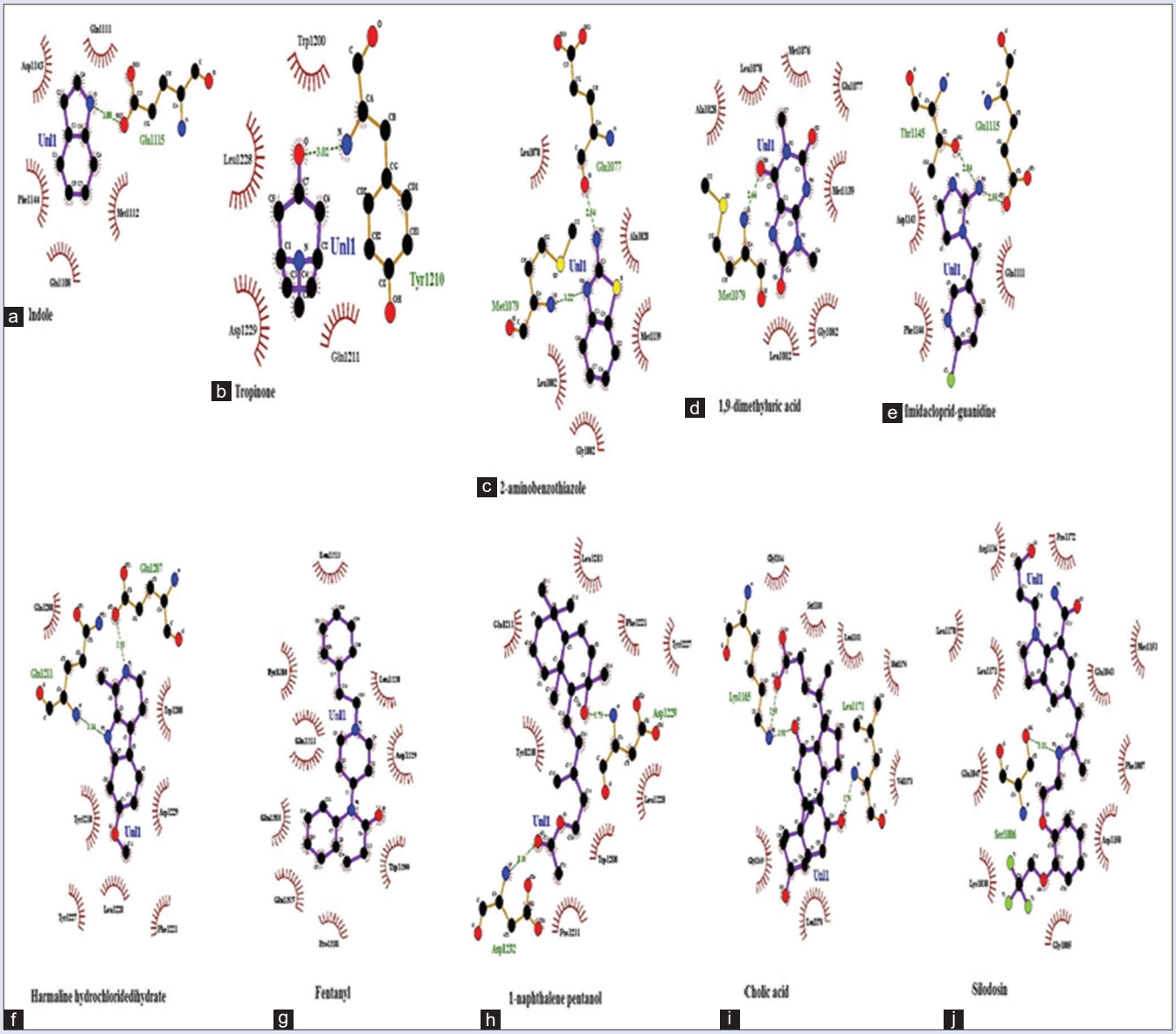

Figure 7: Ligplot analysis results. Interaction was analyzed between insulin receptor and bioactive compounds. (a) Indole, (b) tropinone, (c) 2-aminobenzothiazole, (d) 1,9-dimethyluric acid, (e) imidacloprid–guanidine, (f) harmaline hydrochloride dihydrate, (g) fentanyl, (h) 1-naphthalene pentanol, (i) cholic acid, (j) silodosin

Table 6: Binding energy and active residue site of identified compounds

Ligands	PubChem CID	Binding energy (kcal/mol)	Active residue site
Indole	798	−4.04	GLU1115
Tropinone	79038	−4.5	TYR1210
2-aminobenzothiazole	8706	−4.49	GLU1077
1,9-dimethyluric acid	108712	−4.49	ET1079
Imidacloprid–guanidine	10130527	−5.4	THR1145; GLU1115
Harmaline hydrochloridedihydrate	5280951	−5.51	GLU1207
Fentanyl	3345	−6.09	NO H BONDS
1-naphthalene pentanol	56776325	−5.68	ASP1229
Cholic acid	221493	−6.4	LYS1165; LEU1171
Silodosin	5312125	−2.37	NO H BONDS

CID: Compound identification number

to their pure forms due to the encapsulation of the drug moiety in the polymer matrix.[39]

CONCLUSION

In this study, the synthesis of TC-loaded PLA NPs was optimized by amplitude and sonication time to obtain a high yield percentage. Total alkaloids in TC extract were analyzed by the validation with triple quadrupole LC-MS/MS and FT-IR. The present study proves that TC stem extract possesses a therapeutic effect on diabetes. It is evident that acarbose interaction with insulin receptor shows minimum binding affinity when compared to the compounds predicted from the mass spectrum which shows the highest binding affinity with insulin receptor which acts as an insulin activator and responsible for the inhibitory action of α-glucosidase. Further, the release profile of the TC from the PLA NPs was studied by Higuchi kinetics, and drug transport mechanism showed Fickian diffusion.

Acknowledgements

The authors acknowledge SAIF-CDRI (Lucknow, India) and SAIF-IITM (Chennai, India) for their technical assistance.

Financial support and sponsorship

The authors would like to thank the Vellore Institute of Technology (Vellore, India) for providing the lab facilities and financial assistance.

Conflicts of interest

There are no conflicts of interest.

REFERENCES

1. Saha S, Ghosh S. *Tinospora cordifolia*: One plant, many roles. Anc Sci Life 2012;31:151-9.
2. Dinesh Kumar V, Geethanjali B, Avinash KO, Kumar JR, Chandrashekrappa GK, Basalingappa KM. *Tinospora cordifolia*: The antimicrobial property of the leaves of amruthaballi. J Bacteriol Mycol 2017;5:363-1.
3. Joshi G, Kaur R. *Tinospora cordifolia*: A phytopharmacological review. Int J Pharm Sci Res 2016;7:890-7.
4. Mittal J, Sharma MM, Batra A. *Tinospora cordifolia*: A multipurpose medicinal plant – A review. J Med Plants Stud 2014;2:32-7.
5. Sannegowda KM, Venkatesha SH, Moudgil KD. *Tinospora cordifolia* inhibits autoimmune arthritis by regulating key immune mediators of inflammation and bone damage. Int J Immunopathol Pharmacol 2015;28:521-31.
6. Sharma R, Amin H, Galib, Prajapati PK. Antidiabetic claims of *Tinospora cordifolia* (Willd.) Miers: Critical appraisal and role in therapy. Asian Pac J Trop Biomed 2015;5:68-8.
7. Patel MB, Mishra S. Isoquinoline alkaloids from *Tinospora cordifolia* inhibit rat lens aldose reductase. Phytother Res 2012;26:1342-7.
8. Joshi Y, Bhatt A, Bisht P, Juyal D, Sade S. Evaluation of *Tinospora cordifolia* mucilage as a novel tablet binder. World J Pharm Pharm Sci 2015;4:1113-3.
9. Sultana S, Ali M, Jameel M. Phytochemical investigation and isolation of new compounds from the stems of *Tinospora cordifolia* Miers. Trends Phytochem Res 2017;1:83-2.
10. Oloyede HO, Bello TO, Ajiboye TO, Salawu MO. Antidiabetic and antidyslipidemic activities of aqueous leaf extract of *Dioscoreophyllum cumminsii* (Stapf) diels in alloxan-induced diabetic rats. J Ethnopharmacol 2015;166:313-22.
11. Devulapally R, Paulmurugan R. Polymer nanoparticles for drug and small silencing RNA delivery to treat cancers of different phenotypes. Wiley Interdiscip Rev Nanomed Nanobiotechnol 2014;6:40-60.
12. Zhang S, Wu Y, He B, Luo K, Gu Z. Biodegradable polymeric nanoparticles based on amphiphilic principle: Construction and application in drug delivery. Sci China Chem 2014;57:461-5.
13. Pandey S, Haldar C, Patel D, Maiti P. Biodegradable polymers for potential delivery systems for therapeutics. In: Dutta PK, Dutta J, editors. Multifaceted Development and Application of Biopolymers for Biology, Biomedicine and Nanotechnology. Advances in Polymer Science. Berlin: Springer; 2013. p. 169-202.
14. Weiss CK, Lorenz MR, Landfester K, Mailänder V. Cellular uptake behavior of unfunctionalized and functionalized PBCA particles prepared in a miniemulsion. Macromol Biosci 2007;7:883-96.
15. Chan J, Valencia P, Zhang L, Langer R, Farokhzad O. Polymeric nanoparticles for drug delivery. In: Grobmyer SR, Moudgil BM, editors. Cancer Nanotechnology, Methods in Molecular Biology. Gainesville: Springer Science; 2010. p. 163-75.
16. Danhier F, Ansorena E, Silva JM, Coco R, Le Breton A, Préat V, *et al.* PLGA-based nanoparticles: An overview of biomedical applications. J Control Release 2012;161:505-22.
17. Gou M, Zheng X, Men K, Zhang J, Zheng L, Wang X, *et al.* Poly (epsilon-caprolactone)/poly (ethylene glycol)/poly (epsilon-caprolactone) nanoparticles: Preparation, characterization, and application in doxorubicin delivery. J Phys Chem B 2009;113:12928-33.
18. Kumari A, Yadav SK, Pakade YB, Kumar V, Singh B, Chaudhary A, *et al.* Nanoencapsulation and characterization of *Albizia chinensis* isolated antioxidant quercitrin on PLA nanoparticles. Colloids Surf B Biointerfaces 2011;82:224-32.
19. Zheng X, Kan B, Gou M, Fu S, Zhang J, Men K, *et al.* Preparation of MPEG-PLA nanoparticle for honokiol delivery *in vitro*. Int J Pharm 2010;386:262-7.
20. Majid J, Elmira AT, Muhammad I, Muriel J, Stephane D. Poly-lactic acid: Production, applications, nanocomposites, and release studies. Compr Rev Food Sci Food Saf 2010;9:553-1.
21. Kumari A, Kumar V, Yadav SK. Plant extract synthesized PLA nanoparticles for controlled and sustained release of quercetin: A green approach. PLoS One 2012;7:e41230.
22. Lee SH, Zhang Z, Feng SS. Nanoparticles of poly (lactide)-tocopheryl polyethylene glycol succinate (PLA-TPGS) copolymers for protein drug delivery. Biomaterials 2007;28:2041-50.
23. Pandey SK, Patel DK, Thakur R, Mishra DP, Maiti P, Haldar C. Anti-cancer evaluation of quercetin embedded PLA nanoparticles synthesized by emulsified nanoprecipitation. Int J Biol Macromol 2015;75:521-9.
24. Silva-Buzanello RA, Ferro AC, Bona E, Cardozo-Filho L, Araújo PH, Leimann FV, *et al.* Validation of an ultraviolet-visible (UV-vis) technique for the quantitative determination of curcumin in poly (L-lactic acid) nanoparticles. Food Chem 2015;172:99-104.
25. Joshiand G, Kaur R. *Tinospora cordifolia*: A pharmacological review. Int J Pharm Sci Res 2016;7:890-7.
26. Esmaeilzadeh-Gharedaghi E, Faramarzi MA, Amini MA, Rouholamini Najafabadi A, Rezayat SM, Amani A. Effects of processing parameters on particle size of ultrasound prepared chitosan nanoparticles: An artificial neural networks study. Pharm Dev Technol 2012;17:638-47.
27. Fernández K, Aburto J, von Plessing C, Rockel M, Aspé E. Factorial design optimization and characterization of poly-lactic acid (PLA) nanoparticle formation for the delivery of grape extracts. Food Chem 2016;207:75-85.
28. Kumari A, Yadav SK, Pakade YB, Singh B, Yadav SC. Development of biodegradable nanoparticles for delivery of quercetin. Colloids Surf B Biointerfaces 2010;80:184-92.
29. Shamsa F, Monsel H, Ghamooshi R, Verdian-Rizi M. Sphectrophotometric determination of total alkaloids in some Iranian medicinal plants. Thai J Pharm Sci 2008;32:17.
30. Singh NA, Azad Mandal AK, Khan ZA. Fabrication of PLA-PEG nanoparticles as delivery systems for improved stability and controlled release of catechin. J Nanomaterials 2017;2017:1-9.
31. Costa P, Lobo JMS. Modelling and comparison of dissolution profiles. Eur J Pharm Sci 2011;13:123-3.
32. Dash S, Murthy PN, Nath L, Chowdhury P. Kinetic modeling on drug release from controlled drug delivery systems. Acta Pol Pharm 2010;67:217-23.
33. Telagari M, Hullatti K. *In vitro* α-amylase and α-glucosidase inhibitory activity of *Adiantum caudatum* linn. and *Celosia argentea* linn. Extracts and fractions. Indian J Pharmacol 2015;47:425-9.
34. Jayasree G, Aashish B, Sarfaraz L. Docking studies of Rauwolfia serpentine alkaloids as insulin receptor activators. Int J Comput Appl 2012;43:32-7.
35. Avadi MR, Sadeghi AM, Mohammadpour N, Abedin S, Atyabi F, Dinarvand R, *et al.* Preparation and characterization of insulin nanoparticles using chitosan and Arabic gum with ionic gelation method. Nanomedicine 2010;6:58-63.
36. Kadare P, Maposa P, Dube A, Maponga CC. Encapsulation of isoniazid in chitosan-gum Arabic and poly (lactic-co-glycolic acid) PVA particles to provide a sustained release formulation. J Pharm Pharmacol 2014;S(1):1-6.
37. Ward CW, Lawrence MC. Ligand-induced activation of the insulin receptor: A multi-step process involving structural changes in both the ligand and the receptor. Bioessays 2009;31:422-34.
38. Salatin S, Maleki Dizaj S, Yari Khosroushahi A. Effect of the surface modification, size, and shape on cellular uptake of nanoparticles. Cell Biol Int 2015;39:881-90.
39. Cetin M, Atila A, Sahin S, Vural I. Preparation and characterization of metformin hydrochloride loaded-eudragit®RSPO and eudragit®RSPO/PLGA nanoparticles. Pharm Dev Technol 2013;18:570-6.